Enzyme and Microbial Technology 139 (2020) 109578

Contents lists available at ScienceDirect

Enzyme and Microbial Technology

journal homepage: www.elsevier.com/locate/enzmictec

A voltammetry biosensor based on self-assembled layers of a heteroleptic tris(phthalocyaninato) europium triple-decker complex and tyrosinase for catechol detection

Qi Liu[a,1], Lei Zou[b,1], Qiqi Sun[a], Xiyou Li[a], Yanli Chen[a,*]

[a] School of Materials Science and Engineering, Institute of New Energy, China University of Petroleum (East China), Qingdao 266580, China
[b] Huaneng Weihai Power Generation Co., Ltd., Weihai, 264205, China

ARTICLE INFO

Keywords:
Biosensor
LB films
Catechol
Triphthalocyanine
Tyrosinase

ABSTRACT

A highly efficient enzyme-based sensor was made from a heteroleptic tris(phthalocyaninato) europium triple-decker complex $Eu_2(Pc)[Pc(OPh)_8]_2$, for the first time. The ITO working electrode was modified by a mixture of hybrid multi-layers consisting of $Eu_2(Pc)[Pc(OPh)_8]_2$, stearic acid (SA) and tyrosinase (Tyr) ($Eu_2(Pc)[Pc(OPh)_8]_2$/SA/Tyr-ITO) using the Langmuir-Blodgett (LB) technique. The microstructure and morphology of the resulting LB films can be characterized by their π–A isotherms, UV–vis absorption spectra, X-ray diffraction and atomic force microscopy (AFM) analysis. The experimental results revealed that the triple-decker molecules of $Eu_2(Pc)[Pc(OPh)_8]_2$ take a H-type molecular stacking mode in both pure and mixed LB film, and the microstructures of films were effectively improved by mixing SA within the triple-decker $Eu_2(Pc)[Pc(OPh)_8]_2$ molecules. The excellent electrocatalytic effect of the $Eu_2(Pc)[Pc(OPh)_8]_2$/SA/Tyr LB films, leads to a good linear increase from 5.26×10^{-7} to 2.1×10^{-4} M for catechol. It also leads to an excellent sensitivity of 2.19 μA/μM, and a detection limits of 6.29×10^{-8} M (S/N = 3) of catehol at the oxidation peak, achieving best catechol sensing performance among the phthalocyanine-based biosensing mediators. The reduction peak also showed a good linear increase from 5.26×10^{-7} to 1.60×10^{-4} M for catechol with a sensitivity of 0.615 μA/μM, and a detection limit of 1.69×10^{-7} M (S/N = 3). Moreover, the $Eu_2(Pc)[Pc(OPh)_8]_2$/SA/Tyr-ITO electrode are easy to reproduce, stable and resistant to interference when it comes to detection for catehol, and this indicates great potential of industrial application of tris(phthalocyaninato) rare earth complexes in ultrasensitive and specific biosensors.

1. Introduction

In general, unique electronic characteristics, high chemical stability and great electroactivity of phthalocyanines are well known and documented [1], and as a result, phthalocyanine-based devices have been applied in the electrochemical sensors [2], OFETs [3] and gas sensors [4,5]. Depending on their electroactivity, some electrochemical sensors based on phthalocyanines [6] and biphthalocyanines [7] for the detection of phenolic compounds have been researched widely. Very recently, solution-processed quasi-Langmuir–Shäfer (QLS) films of the functionalized sandwich mixed (phthalocyaninato) (porphyrinato) europium derivatives have been revealed to display specific electrochemical recognition for H_2O_2 [8], dopamine, uric acid, tyrosine, tryptophan and acetaminophen [9,10], etc. depending mainly on intermolecular interaction between triple-deckers and the analytes. However, to the best of our knowledge an electrochemical sensor based on tris(phthalocyaninato) rare earth triple-deckers towards catechol has not yet been reported.

Catechol is a phenolic compound which is widely used in many chemical industries for the production of pesticides, plastics, herbicides, pharmaceuticals, cosmetics, antiseptics and synthetic products. Nevertheless, catechol is also a toxic environmental pollutant due to its poor biodegradability in waste water [11]. Up to now,many kinds of methods have been used for the determination of catechol, such as flow injection analysis [12], electrochemical methods [13], high performance liquid chromatography (HPLC) [14], electro-chemiluminescence [15], and gas chromatography/mass spectrometry [16]. However, the practical applications of these methods still have some limitations such as complicated operating conditions, time-consuming processes, expensive equipment, etc. Therefore, much efforts have been devoted to

* Corresponding author.
E-mail address: yanlichen@upc.edu.cn (Y. Chen).
[1] These authors contributed equally.

https://doi.org/10.1016/j.enzmictec.2020.109578
Received 26 October 2019; Received in revised form 10 April 2020; Accepted 11 April 2020
Available online 04 May 2020

develope the simple, sensitive, and cost-effective electrochemical method for detection of catechol. It has been reported that catechol can be detected by using the DMPA (phospholipid dimyristoyl phosphatidic acid) mixed either with FePc (iron phthalocyanine) or with $LuPc_2$ (lutetium bisphthalocyanine) as voltammetry sensors, achieving the limit of detection (LOD) of 4.30×10^{-7} and 3.34×10^{-7} M for FePc/DMPA and $LuPc_2$/DMPA, respectively [17]. The biomimetic sensors containing $LuPc_2$ and tyrosinase nano-aggregates was developed for the voltammetry detection of catechol with a LOD as low as 3.75×10^{-7} M [18]. By using CoPc as an electron mediator and tyrosinase as a biocatalyst, the-CoPc/tyrosinase-based sensor exhibited a highly sensitive response to catechol with a low LOD of 1.66×10^{-6} M [19]. Compared to metal phthalocyanines (MPcs) and bis(phthalocyaninato) rare earth double-decker complexes, tris(phthalocyaninato) rare earth triple-decker complexes possess more extended systems in the normal direction of the macrocycle plane. Therefore, it would be high promising for these triple-deckers as electroactive candidates in electrochemical sensing application [8–10]. With this background in mind, herein, the self-assemblied hybrid films of a tris(phthalocyaninato)europium(III) complex, $Eu_2Pc[Pc(OPh)_8]_2$ [Pc = unsubstituted phthalocyaninate; Pc $(OPh)_8$ = 2,3,9,10,16,17,23,24-octaphenoxyphthalocyaninate] (Scheme 1), mixed with stearic acid (SA) (denoted as $Eu_2Pc[Pc(OPh)_8]_2$)/SA are prepared by using the Langmuir-Blodgett (LB) technique. The sensitive and selective electrochemical responses of the $Eu_2Pc[Pc(OPh)_8]_2$)/SA LB films modified by tyrosinase (Tyr) toward catechol have been revealed.

2. Experimental section

2.1. Fabrication of $Eu_2Pc[Pc(OPh)_8]_2$)/SA and $Eu_2Pc[Pc(OPh)_8]_2$)/SA/Tyr films

To prepare $Eu_2Pc[Pc(OPh)_8]_2$)/SA films, a mixed solution of $Eu_2Pc[Pc(OPh)_8]_2$ and stearic acid (SA) in a molar ratio of 1:5 dissolved in chloroform (1×10^{-4} M) acted as the spread sample and ultrapure water as the subphase. LB hybrid films of $Eu_2Pc[Pc(OPh)_8]_2$/SA were deposited onto ITO glass substrates under the surface pressure of 20 mN m^{-1}.

In order to immobilize tyrosinase on the resulting LB films, the $Eu_2Pc[Pc(OPh)_8]_2$/SA LB films (20-layers)-modified ITO electrode was firsly activated by immersing in the mixed solution of 5 mM NHS and 2 mM EDC for 1 h. After rinse with deionized water, the activated ITO electrode n was immersed into the PBS solution containing 280 μg ml^{-1} tyrosinase for 1 day followed by drying in air at room temperature to form $Eu_2Pc[Pc(OPh)_8]_2$/SA/Tyr films.

The other experimental details including materials, chemicals, apparatus and measuremental methods are shown in the Supporting information.

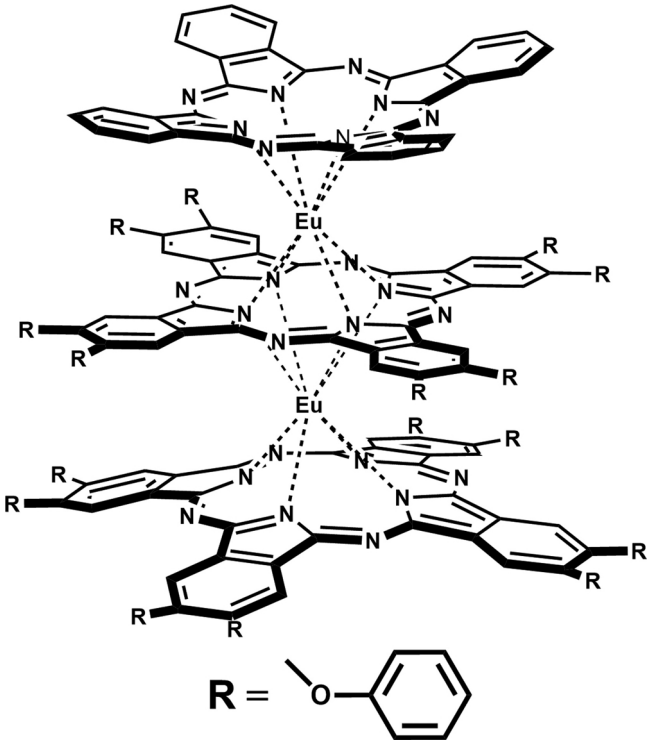

Scheme 1. Schematic molecular structure oftris(phthalocyaninato) europium triple-decker complex $Eu_2Pc[Pc(OPh)_8]_2$.

3. Results and discussion

3.1. Film morphology and microstructure

The pressure–surface area (π–A) isotherms of pure triple-deckers and their mixtures with stearic acid (SA) in a molar ratio of 1:5 were comparatively studied for the evaluation of the molecular packing behaviors triple-deckers $Eu_2(Pc)[Pc(OPh)_8]_2$ molecules on the air/water interface, Fig. 1. A molar ratio of 1:5 was chosen as it allows for the incorporation of SA without compromising the electrochemical chemical properties of the triple-deckers, meanwhile enough carboxyl groups from SA in the mixed LB films were expected to effectively immobilize Tyr species. As can be seen, the collapseing pressure of mixed monolayer of $Eu_2(Pc)[Pc(OPh)_8]_2$/SA (~32 mN/m) is higher than that of corresponding pure $Eu_2(Pc)[Pc(OPh)_8]_2$ monolayer (~25 mN/m), implying superior stability and film-forming ability for the mixed $Eu_2Pc[Pc(OPh)_8]_2$/SA monolayer on pure water subphase. The limiting molecular areas of 0.44 and 1.60 nm^2 per molecule were obtained for the mixed and pure monolayer of $Eu_2(Pc)[Pc(OPh)_8]_2$, respectively. By means of the closely packed molecular area of SA, 0.21 nm^2 (Fig. 1), a limiting molecular area ($A_{limit(mixture)} = 1/6A_{calcd\ (pure)} + 5/6A_{SA}$) of pure $Eu_2(Pc)[Pc(OPh)_8]_2$ is estamited to be ca.1.59 nm^2/molecule if an ideal $Eu_2(Pc)[Pc(OPh)_8]_2$/SA mixture formed in the resulting hybrid monolayer. This value is in good agreement with that obtained by experiment (1.60 nm^2/molecule), implying that the incorporation of SA molecules into the hybrid monolayers have no effect on the orientation of the phthalocyanine molecules [20–22]. However, the average area per molecule of $Eu_2(Pc)[Pc(OPh)_8]_2$ in pure and mixed films is much smaller than that of either the projection for a perpendicular standing molecule of $Eu_2(Pc)[Pc(OPh)_8]_2$ (ca. 2.7 nm^2/molecule), or a molecular planar area with the

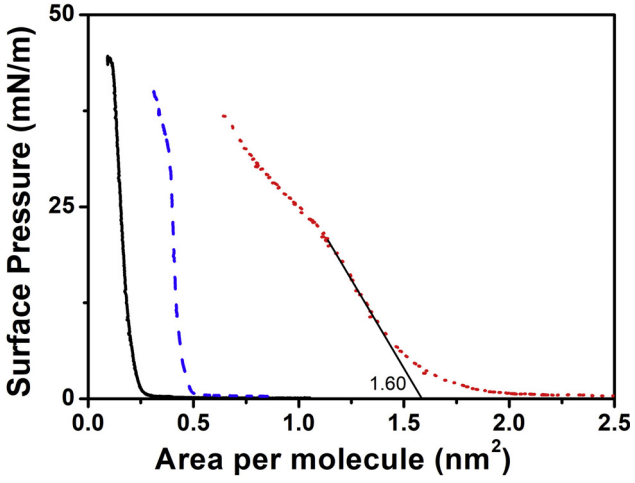

Fig. 1. π–A isotherms of SA (solid line), $Eu_2Pc[Pc(OPh)_8]_2$ (dash line) and $Eu_2Pc[Pc(OPh)_8]_2$/SA (1:5) (dot line) both at the air–pure water interface.

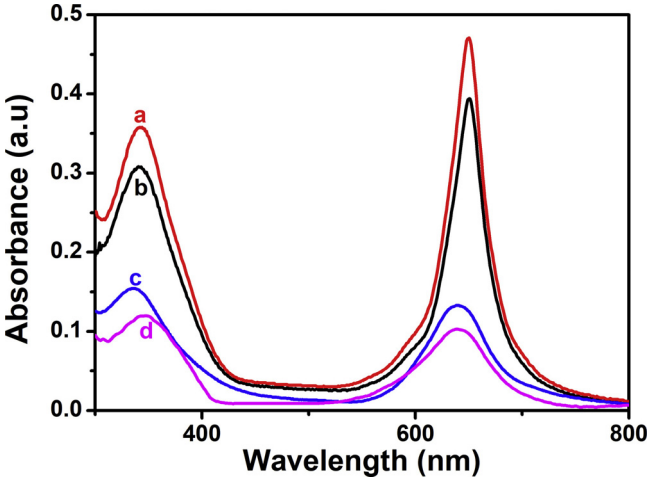

Fig. 2. UV–vis absorption spectra of (a) $Eu_2Pc[Pc(OPh)_8]_2$ and (b) mixed $Eu_2Pc[Pc(OPh)_8]_2$/SA in $CHCl_3$, (c) pure $Eu_2Pc[Pc(OPh)_8]_2$ and (d) $Eu_2Pc[Pc(OPh)_8]_2$/SA mixed LB films.

phthalocyanine ring plane facing on water surface (ca. 4.4 nm^2 /molecule), based on the diagonal dimension (2.1 nm) and thickness (1.3 nm) of $Eu_2(Pc)[Pc(OPh)_8]_2$ taken from single crystal X-ray diffraction results [23]. Therefore, it is deduced that $Eu_2(Pc)[Pc(OPh)_8]_2$ molecules stacked closely with a "face-to-face" configuration (H-aggregation) in the monolayers, where there were longitudinal overlaps between phenoxy substituents from adajacent triple-decker molecules owing to the strong π-π stacking and hydrophobic interactions among both the phthalocyanine rings and the phenoxy substituents of triple-decker molecules.

The absorption maxima from the UV–vis spectra of the $CHCl_3$ solution and the LB films for $Eu_2(Pc)[Pc(OPh)_8]_2$ and $Eu_2(Pc)[Pc(OPh)_8]_2$/SA are recorded in Fig. 2. As can be seen, an intense Q band appeared at ca. 650 nm for $Eu_2Pc[Pc(OPh)_8]_2$ in $CHCl_3$, Fig. 2a. However, a blue-shifted Q band at 640 nm was found for $Eu_2(Pc)[Pc(OPh)_8]_2$ in both the pure and mixed films, suggesting H-aggregates formed for the triple-deckers in the LB films, according to exciton theory [24] and previously research [20,25,26]. Furthermore, the spectra for $Eu_2(Pc)[Pc(OPh)_8]_2$ in pure and mixed LB films are very similar in terms of both the peak position and the band width, indicates that the aggregation mode of the $Eu_2(Pc)[Pc(OPh)_8]_2$ molecules in the LB films were not affected by the SA, being preserved upon transfer onto a solid support as in the LB film,which is consistent with the the previous literature studies on sandwich bis-and tris(phthalocyaninato) rare earth analogues [21,22].

The LB films were further evaluated by X-ray diffraction (XRD). The pure $Eu_2Pc[Pc(OPh)_8]_2$ and $Eu_2Pc[Pc(OPh)_8]_2$/SA mixed LB films show obvious diffraction peaks in the low-angle region, Fig. 3, demonstating an uniform orientation of the triple-decker molecules relative to the plane of the substrate in a layered structure. The (001) Bragg diffraction peak at $2\theta = 4.42^\circ$ and 4.36° for the pure and mixed LB films, respectively, corresponds to a regualr distance of 1.99 and 2.04 nm. As a result, orientation angles of phthalocyanine rings with respect to the substrate are estimated to be ca. 71° and 76° for $Eu_2Pc[Pc(OPh)_8]_2$ in the pure and mixed LB films (the inset of Fig. 3A and B), based on the diagonal dimension of $Eu_2(Pc)[Pc(OPh)_8]_2$ (2.1 nm) [19]. However, anothor well-defined peak is observed at $2\theta = 2.06^\circ$ for the $Eu_2Pc[Pc(OPh)_8]_2$/SA mixed film, providing a layer space of ca. 4.29 nm. Consequently, the Y-type LB film formed for the SA molecules with a slight mutual penetration between the alkyl chains [21], which further confirmed SA molecules have been introduced into the LB films of $Eu_2Pc[Pc(OPh)_8]_2$/SA.

The morphologies of $Eu_2Pc[Pc(OPh)_8]_2$ and $Eu_2Pc[Pc(OPh)_8]_2$/SA films were characterized by AFM. As presented in Fig. 4A, $Eu_2Pc[Pc(OPh)_8]_2$ film showed a sheetlike structure comtaning some aggregate domains on the surface of the film. However, after being fabricated into $Eu_2Pc[Pc(OPh)_8]_2$/SA film, two different phases (i.e.bright and dark nanoparticles) were observed, in which uniform granular crystallites formed on the suface of the mixed films in contrast to the randomly dispersed domains in the pure film, Fig. 4B. These are expected to be beneficial for the electrocatalytic activity of $Eu_2Pc[Pc(OPh)_8]_2$/SA films for electrochemical sensing applications [8].

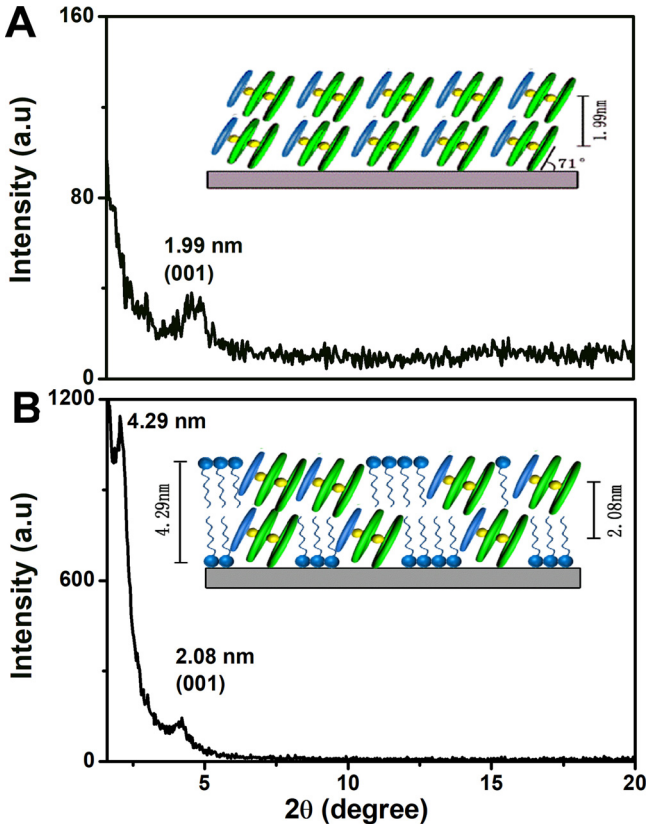

Fig. 3. X-ray diffraction patterns of the LB films of $Eu_2Pc[Pc(OPh)_8]_2$ (A) and $Eu_2Pc[Pc(OPh)_8]_2$/SA (B). The insets show the possible molecular organization on ITO surface.

3.2. The analysis of the electrochemical sensor

The electrochemical response of bare ITO electrode, an ITO covered with $Eu_2Pc[Pc(OPh)_8]_2$/SA mixted films ($Eu_2Pc[Pc(OPh)_8]_2$/SA-ITO) and $Eu_2Pc[Pc(OPh)_8]_2$/SA absorbing with tyrosinase ($Eu_2Pc[Pc(OPh)_8]_2$/SA/Tyr-ITO) were tested *via* immersing the electrodes towards catechol (10^{-5} M) in 0.01 M phosphate buffer solution pH = 7.0 at 0.02 V s^{-1} (Fig. 5).The diverse responses of the three electrodes can disclose some valuable clues about the effects of the electronic media of the $Eu_2Pc[Pc(OPh)_8]_2$ and the enzymatic activity [18]. The voltammograms in PBS using bare ITO immersed in catechol solution (10^{-5} M) exhibits one cathodic (reduction) peak at −0.235 V, Fig. 5a, which is in accordance with that found in the literature [24,27]. However, the anodic peak for the ITO in catechol solution (10^{-5} M) related to the electrochemical oxidation of the catechol cannot be observed, which is likely due to the very low concentration of catechol employed [17]. The CV response of the $Eu_2Pc[Pc(OPh)_8]_2$/SA-ITO electrode towards catechol (10^{-5} M) showed a significant peak at 0.498 V (peak I), assigned to the electrochemical oxidation of the catechol [28], Fig. 5b. This is lower than the oxidation of the catechol occuring by using a carbon paste electrode [29,30]. Consequently, the existence of $Eu_2Pc[Pc(OPh)_8]_2$ boosted the oxidation of catechol, thus confirming an electrocatalytic effect of the $Eu_2Pc[Pc(OPh)_8]_2$. In the case of $Eu_2Pc[Pc$

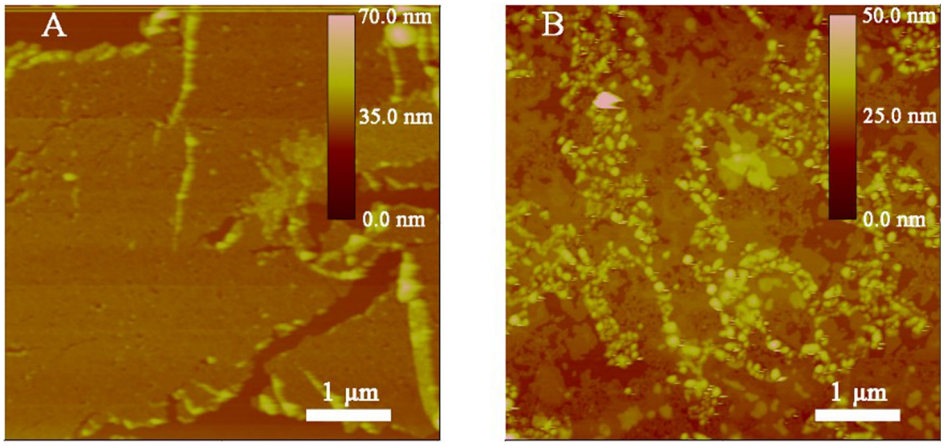

Fig. 4. AFM images of $Eu_2Pc[Pc(OPh)_8]_2$ (A) and $Eu_2Pc[Pc(OPh)_8]_2$/SA (B) films.

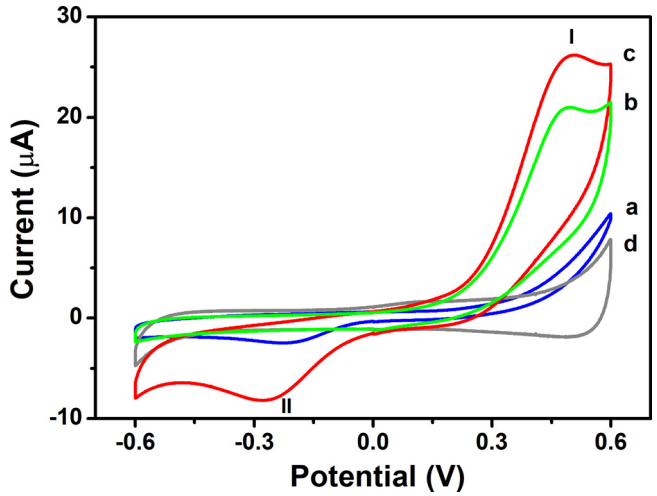

Fig. 5. Cyclic voltammograms of bare ITO electrode (a), $Eu_2Pc[Pc(OPh)_8]_2$/SA-ITO (b), $Eu_2Pc[Pc(OPh)_8]_2$/SA/Tyr-ITO (c) immersed in 0.01 M phosphate buffer (PBS, pH = 7.0) with 10^{-5} M catechol acid, and $Eu_2Pc[Pc(OPh)_8]_2$/SA/Tyr-ITO immersed in 0.01 M PBS without catechol (d), respectively, at scan rate of 0.02 V s^{-1}.

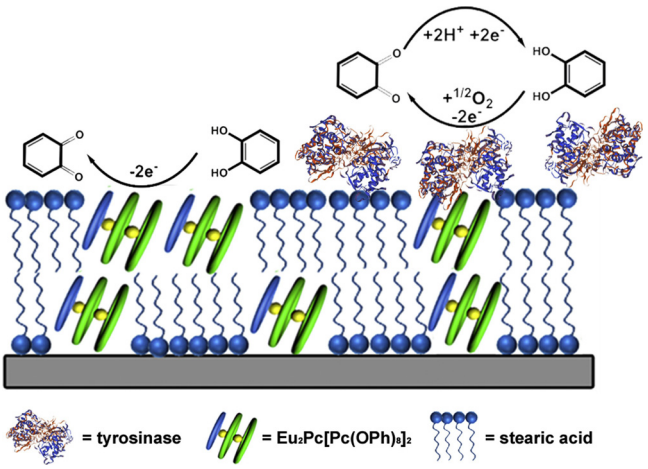

Fig. 6. Schematic illustration of the reactions that take place at the $Eu_2Pc[Pc(OPh)_8]_2$/SA/Tyr-ITO biosensor surface.

$(OPh)_8]_2$/SA/Tyr-ITO electrode, the voltammetric response towards catechol (10^{-5} M) exhibited two definite redox processes, Fig. 5c. One well-defined cathodic peak at −0.271 V (peak II) related to the reduction of the *o*-quinone to catechol that occurs upon absorption of tyrosinase, and another electrochemical oxidation peak appeared at 0.498 V (peak I) [31]. Furthermore, the presence of tyrosinase on the $Eu_2Pc[Pc(OPh)_8]_2$/SA/Tyr-ITO surface also increases drastically the intensity of oxidation peak (peak I) involving the electrocatalytic activity of $Eu_2Pc[Pc(OPh)_8]_2$ compared to that of $Eu_2Pc[Pc(OPh)_8]_2$/SA-ITO, revealing the interaction between the $Eu_2Pc[Pc(OPh)_8]_2$ and the enzyme and its subsequent electrocatalytic effect. This is in accord with the case of $LuPc_2$ reported by Rodriguez-Mendez et al. [18]. Note that, the voltammogram registered in PBS using $Eu_2Pc[Pc(OPh)_8]_2$/SA/Tyr-ITO electrode without catechol showed only a small background current, Fig. 5d.

On the basis of the present experimental results, the response mechanism of the $Eu_2Pc[Pc(OPh)_8]_2$/SA/Tyr-ITO towards catechol was proposed and shown in Fig. 6. The coupling of the oxidation of catechol to the *o*-quinone (peak I) facilitated by the $Eu_2Pc[Pc(OPh)_8]_2$ and the reduction of the *o*-quinone(peak II) produced by enzymatic oxidation forms a reaction cycle, resulting in signal amplification. Kinetic studies were studied by recording the CVs of the $Eu_2Pc[Pc(OPh)_8]_2$/SA/Tyr-ITO biosensor at different scan rate, from 0.02 to 0.2 V s^{-1} in 10^{-5} M catechol solution (Fig. S1A). Both the anodic and cathodic peak currents (denoted as I_{pa} and I_{pc}) of catechol are proportional to the square root of the scan rate in Fig. S1B, demonstrating a surface diffusion-controlled process for catechol at the $Eu_2Pc[Pc(OPh)_8]_2$/SA/Tyr-ITO electrode [32].

The CVs responses of $Eu_2Pc[Pc(OPh)_8]_2$/SA/Tyr-ITO to the varied concentrations of catechol were investigated by exposing the electrode in 0.526–210 μM catechol solution. As can be seen from Fig. 7A, the intensity of both electrochemical oxidation (peak I) and the enzymatic process (peak II) increased with inceased catechol concentration. A linear response with sensitivity of 2.19 μA/μM for oxidation peak (peak I) was observed in the range of 0.526–210 μM (R^2 = 0.9932), while a narrower linear range from 0.526 to 100 μM (R^2 = 0.999) with lower sensitivity of −0.615 μA/μM was obtained for the enzymatic process (peak II), in Fig. 7B. The more efficient solid-state packing effect and a large number of electroactive species supported by $Eu_2Pc[Pc(OPh)_8]_2$ molecules than those by enzyme in the $Eu_2Pc[Pc(OPh)_8]_2$/SA/Tyr film modified on the surface of ITO should favor charge transfer in LB film and through electrode interface, which led to an increased sensitivity obtained from electrochemical oxidation. According to the $3S_b/m$ equation [m = the slope of the calibration plot, S_b = the standard deviation (n = 6) of the amperometric signals of the blank at the potential measured [33], the corresponding LOD were calculated to be 0.187 μM for the electrochemical process (peak I) and 0.324 μM for the enzymatic process (peak II), respectively, being in polyphenol range of concentrations found in water, foods and others [34].

The relationship between the peak current of the $Eu_2Pc[Pc$

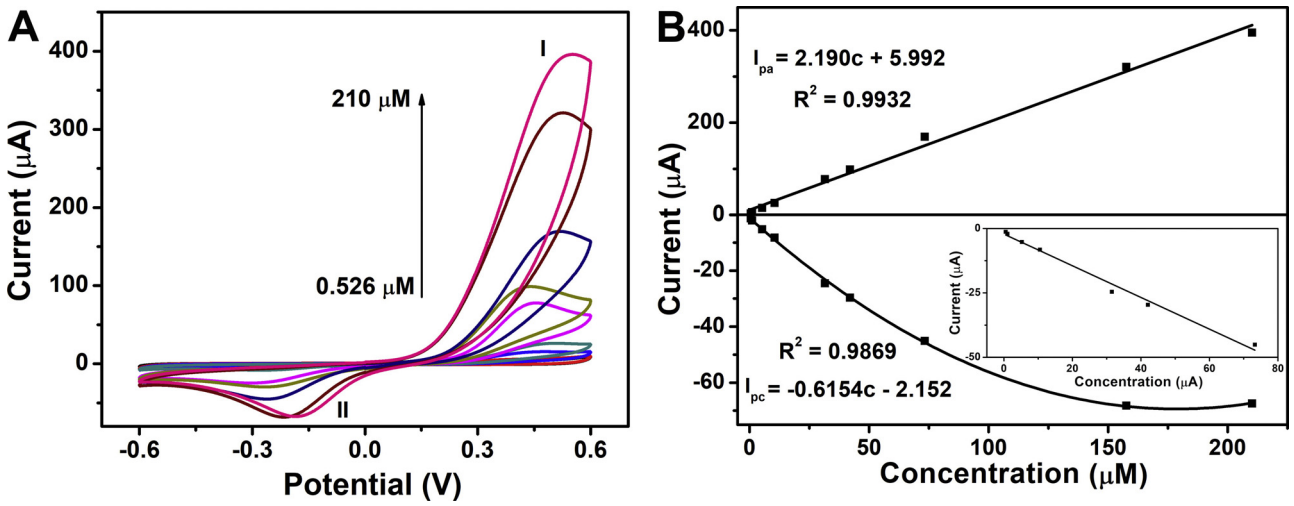

Fig. 7. (A) Cyclic voltammograms response of $Eu_2Pc[Pc(OPh)_8]_2$/SA/Tyr-ITO to different concentration of catechol (0.526–210 μM) in pH = 7.0 PBS. (B) Oxidation peak intensity and reduction peak intensity *vs* catechol concentration. Plot of the relationship between reduction peak intensity and catechol concentration (0.526–80 μM).

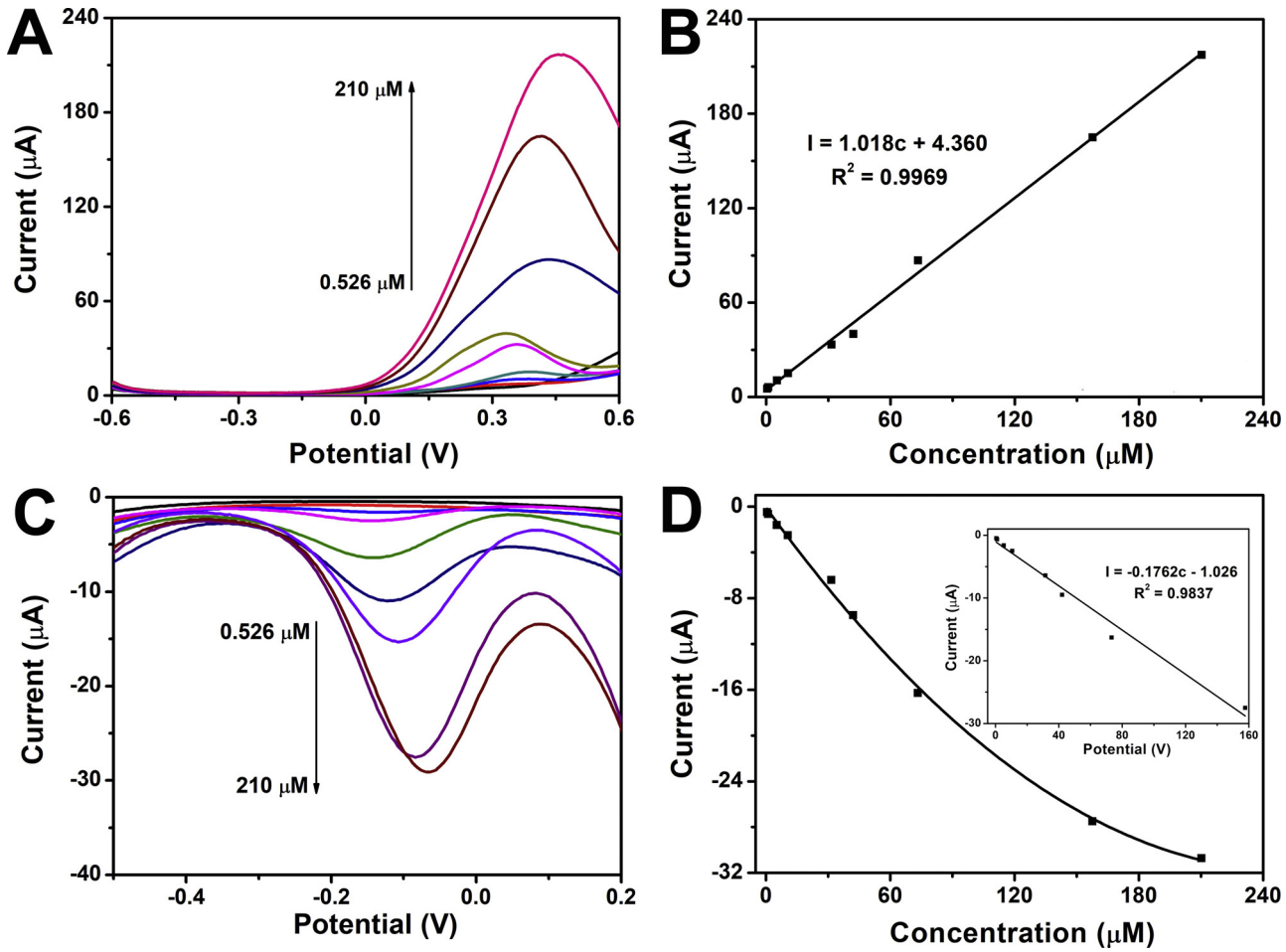

Fig. 8. DPV responses and the corresponding peak intensity vs. concentration of catechol in the range of 0.526–210 μM: oxidation peak (A and B) and reduction peak (C and D). The inset of D shows a linear plot between reduction peak intensity and concentration of catechol in 0.526–160 μM range, at $Eu_2Pc[Pc(OPh)_8]_2$/SA/Tyr-ITO electrode in 0.1 M phosphate buffer (pH = 7.0).

$(OPh)_8]_2$/SA/Tyr-ITO sensor and concentration of catechol has also been further assessed using differential pulse voltammetry (DPV) technique for comparison, Fig. 8. As shown in Fig. 8A and 8C, the changes in the currents of both anodic and cathodic peaks corresponding to the electrochemical oxidation and enzymatic processes clearly disclose the good separation of the different catechol concentration levels in 0.526 ~ 210 μM range. The corresponding DPV calibration sets of both anodic and cathodic peaks were collected (Fig. 8B and D). Similar to those from CV response, the intensity of peak current enhanced linearly with increasing in the catechol concentration from

0.526 to 210 μM with a sensitivity of 1.018 μA/μM for anodic peak [I_p (μA) = 4.360 + 1.018c (μM), R^2 = 0.9969] and from 0.526 μM to 158 μM with a sensitivity of 0.1616 μA/μM for cathodic peak [I_p (μA) = −1.296 to 0.1616c (μM), (R^2 = 0.9891)], respectively. The LOD was 0.0629 μM and 0.169 μM for anodic and cathodic peak, respectively. As expected, a significant lower LOD to catechol, particularly from the anodic peak, has been achieved by DPV than those by CV. Each data point represents the average of three separate measurements with three different modified ITO for a single phenol concentration. Note that the LOD of 0.0629 μM from anodic peak in the present case was almost one order of magnitude lower than those reported for a biosensor based on tyrosinase and bisphthalocyanine [32], and 26 times lower than the value found in Tyr/CoPc-CNTP [17], indicating promising application of tris(phthalocyaninato) rare earth triple-deckers for biosensors. The performance of $Eu_2Pc[Pc(OPh)_8]_2$/SA/Tyr-ITO sensor was compared with the results reported in the previous literature using Tyr based electrochemical sensors for the detection of catechol in Table S1 (SI). As far as we know, this result represents the best sensing performance for detecting catechol among the phthalocyanine-based molecular materials as biosensing mediators.

3.3. Reproducibility, stability and interference

The relative standard deviation (RSD) of peak currents was calculated to be ~3.9% for cathodic peak and 5.4% for anodic peak upon 6 electrodes, revealing the excellent reproducibility of the $Eu_2Pc[Pc(OPh)_8]_2$/SA/Tyr-ITO electrode (Fig. S2). In addition, for measuring the long-term stability, the $Eu_2Pc[Pc(OPh)_8]_2$/SA/Tyr-ITO was evaluated in 0.1 M PBS buffer (pH = 7.0) containing 10^{-5} M catechol. The athodic peak current decreased less than 2.69% for storing 7 days, (Fig. S3), suggesting that the good stability. The specificity of the developed sensor is also investigated. As shown in Fig. S4, the cyclic voltammograms signal of $Eu_2Pc[Pc(OPh)_8]_2$/SA/Tyr-ITO for 30 μM catechol showed a negligible change upon other six molecules including caffeic acid, citric acid, phenol, arginine, glucose and histidine at 30 μM. confirming the high selectivity to catechol for the present sensor.

4. Conclusions

An enzymatic electrochemical sensor based on Tyrosinase and a triple-decker has been developed for the first time. The great electroactivity and the conductive nature of the triple-decker combined with highly selective catalysis of tyrosinase presents $Eu_2Pc[Pc(OPh)_8]_2$/SA/Tyr-ITO outstanding sensing properties to catechol, representing advanced level among the enzymatic organic semiconductor-based biosensors. This work provides a promising way toward developing highly stable, ultrasensitive electrochemical sensors by making use of both the selective catalysis of tyrsinase enzymatics and the great electroactivity of phthalocyaninato europium triple-deckers.

CRediT authorship contribution statement

Qi Liu: Investigation, Formal analysis, Writing - original draft. **Lei Zou:** Data curation, Writing - original draft. **Qiqi Sun:** Investigation. **Xiyou Li:** Funding acquisition. **Yanli Chen:** Supervision, Writing - review & editing.

Acknowledgements

This work was financially supported by the National Natural Science Foundation of China (No. 21771192), the Natural Science Foundation of Shandong Province (No. ZR2017ZB0315, ZR2017MB006), Postgraduate's Innovation Project (No. YCX2019070), Fundamental Research Funds for the Central Universities (No. 18CX06001A, 19CX05001A) and X. Li thank Taishan Scholar program of Shandong Province for the financial support (ts201712019).

Appendix A. Supplementary data

Supplementary material related to this article can be found, in the online version, at doi:https://doi.org/10.1016/j.enzmictec.2020.109578.

References

[1] Z. Liu, A.A. Yasseri, J.S. Lindsey, D.F. Bocian, Molecular memories that survive silicon device processing and real-world operation, Science 302 (2003) 1543–1545.
[2] S. Chaiyo, E. Mehmeti, W. Siangproh, T.L. Hoang, H.P. Nguyen, O. Chailapakul, K. Kalcher, Non-enzymatic electrochemical detection of glucose with a disposable paper-based sensor using a cobalt phthalocyanine–ionic liquid–graphene composite, Biosens. Bioelectron. 102 (2018) 113–120.
[3] Z. Bao, A.J. Lovinger, J. Brown, New air-stable n-channel organic thin film transistors, J. Am. Chem. Soc. 120 (1998) 207–208.
[4] A.R. Jalil, H. Chang, V.K. Bandari, P. Robaschik, J. Zhang, P.F. Siles, G. Li, D. Bürger, D. Grimm, X. Liu, Fully integrated organic nanocrystal diode as high performance room temperature NO_2 sensor, Adv. Mater. 28 (2016) 2971–2977.
[5] A. Rydosz, E. Maciak, K. Wincza, S. Gruszczynski, Microwave-based sensors with phthalocyanine films for acetone, ethanol and methanol detection, Sens. Actuators B 237 (2016) 876–886.
[6] Z. Zeng, X. Fang, W. Miao, Y. Liu, T. Maiyalagan, S. Mao, Electrochemically sensing of trichloroacetic acid with iron (II) phthalocyanine and Zn-based metal organic framework nanocomposites, ACS Sens. 4 (2019) 1934–1941.
[7] P. Gaudillat, A. Wannebroucq, J.-M. Suisse, M. Bouvet, Bias and humidity effects on the ammonia sensing of perylene derivative/lutetium bisphthalocyanine MSDI heterojunctions, Sens. Actuators B 222 (2016) 910–917.
[8] Z. Yu, L. Zou, Y. Chen, J. Jiang, (Pc) Eu (Pc) Eu [trans-T ($COOCH_3$)$_2$PP]/GO hybrid film-based nonenzymatic H_2O_2 electrochemical sensor with excellent performance, ACS Appl. Mater. Interfaces 8 (2016) 30398–30406.
[9] J. Dong, Z. Yu, X. Kong, S. Zhao, X. Li, Y. Chen, J. Jiang, A calix[4]arene-modified (Pc)Eu(Pc)Eu[T(C4A)PP]-based sensor for highly sensitive and specific host–guest electrochemical recognition, Dalton Trans 48 (2019) 718–727.
[10] Q. Cheng, H. Wang, Y. Wu, S. Zhao, X. Kong, Y. Chen, J. Jiang, Highly selective enzymatic-free electrochemical sensor for dopamine detection based on the self-assemblied film of a sandwich mixed (phthalocyaninato)(porphyrinato)europium derivative, J. Porphyrins Phthalocyanines 21 (2017) 796–802.
[11] J. Healy, L. Young, Catechol and phenol degradation by a methanogenic population of bacteria, Appl. Environ. Microbiol. 35 (1978) 216–218.
[12] J.A. Garcia-Mesa, R. Mateos, Direct automatic determination of bitterness and total phenolic compounds in virgin olive oil using a pH-based flow-injection analysis system, J. Agric. Food. Chem. 55 (2007) 3863–3868.
[13] Y. Liu, R. Wang, Y. Zhu, R. Li, J. Zhang, Photoelectrochemical sensing of catechol based on CdS-DNA-pristine graphene nanocomposite film, Sens. Actuators B 210 (2015) 355–361.
[14] A. Asan, I. Isildak, Determination of major phenolic compounds in water by reversed-phase liquid chromatography after pre-column derivatization with benzoyl chloride, J. Chromatogr. A 988 (2003) 145–149.
[15] Q. Lu, H. Hu, Y. Wu, S. Chen, D. Yuan, R. Yuan, An electrogenerated chemiluminescence sensor based on gold nanoparticles@ C60 hybrid for the determination of phenolic compounds, Biosens. Bioelectron. 60 (2014) 325–331.
[16] E.L.B. Lourenço, A. Ferreira, E. Pinto, M. Yonamine, S.H.P. Farsky, On-fiber derivatization of SPME extracts of phenol, hydroquinone and catechol with GC-MS detection, Chromatographia 63 (2006) 175.
[17] P. Alessio, F.J. Pavinatto, O.N. Oliveira Jr, J.A.D.S. Saez, C.J. Constantino, M.L. Rodríguez-Méndez, Detection of catechol using mixed Langmuir–Blodgett films of a phospholipid and phthalocyanines as voltammetric sensors, Analyst 135 (2010) 2591–2599.
[18] E.G.R. Fernandes, L.C. Brazaca, M.L. Rodríguez-Mendez, J.A. de Saja, V. Zucolotto, Immobilization of lutetium bisphthalocyanine in nanostructured biomimetic sensors using the LbL technique for phenol detection, Biosens. Bioelectron. 26 (2011) 4715–4719.
[19] I. Apetrei, M. Rodriguez-Mendez, C. Apetrei, J. De Saja, Enzyme sensor based on carbon nanotubes/cobalt (II) phthalocyanine and tyrosinase used in pharmaceutical analysis, Sens. Actuators B 177 (2013) 138–144.
[20] D. Li, H. Wang, J. Kan, W. Lu, Y. Chen, J. Jiang, H-aggregation mode in triple-decker phthalocyaninato-europium semiconductors. Materials design for high-performance air-stable ambipolar organic thin film transistors, Org. Electron. 14 (2013) 2582–2589.
[21] Y. Chen, Y. Zhang, P. Zhu, Y. Fan, Y. Bian, X. Li, J. Jiang, Arrangement of tris (phthalocyaninato) gadolinium triple-decker complexes with multi-octyloxy groups on water surface, J. Colloid Interface Sci. 303 (2006) 256–263.
[22] L. Gaffo, C. Constantino, W. Moreira, R. Aroca, O. Oliveira, Atomic force microscopy and micro-Raman imaging of mixed Langmuir-Blodgett films of ytterbium bisphthalocyanine and stearic acid, Langmuir 18 (2002) 3561–3566.
[23] Y. Chen, W. Su, M. Bai, J. Jiang, X. Li, Y. Liu, L. Wang, S. Wang, High performance organic field-effect transistors based on amphiphilic tris (phthalocyaninato) rare earth triple-decker complexes, J. Am. Chem. Soc. 127 (2005) 15700–15701.
[24] M. Kasha, H. Rawls, M. El-Bayoumi, The exciton model in molecular spectroscopy, Pure Appl. Chem. 11 (1965) 371–392.
[25] G. Lu, Y. Chen, Y. Zhang, M. Bao, Y. Bian, X. Li, J. Jiang, Morphology controlled self-assembled nanostructures of sandwich mixed (phthalocyaninato)

(porphyrinato) europium triple-deckers. Effect of hydrogen bonding on tuning the intermolecular interaction, J. Am. Chem. Soc. 130 (2008) 11623–11630.
[26] Y. Chen, R. Li, R. Wang, P. Ma, S. Dong, Y. Gao, X. Li, J. Jiang, Effect of peripheral hydrophobic alkoxy substitution on the organic field effect transistor performance of amphiphilic tris (phthalocyaninato) europium triple-decker complexes, Langmuir 23 (2007) 12549–12554.
[27] S. Casilli, M. De Luca, C. Apetrei, V. Parra, Á.A. Arrieta, L. Valli, J. Jiang, M.L. Rodríguez-Méndez, J.A. De Saja, Langmuir–Blodgett and Langmuir–Schaefer films of homoleptic and heteroleptic phthalocyanine complexes as voltammetric sensors: applications to the study of antioxidants, Appl. Surf. Sci. 246 (2005) 304–312.
[28] B. Khalid, A. Rahim, M.A. Gilani, N. Muhammad, A.R. Younus, S. Tabassum, J. Iqbal, A.I. Alharthi, In situ immobilization of CuO on SiO_2/graphite matrix, modified with benzimidazolium-1-acatate ionic liquid: application as catechol sensor, J. Mol. Liq. 251 (2018) 450–457.
[29] O. Makhotkina, P.A. Kilmartin, The use of cyclic voltammetry for wine analysis: determination of polyphenols and free sulfur dioxide, Anal. Chim. Acta 668 (2010) 155–165.
[30] C. Medina-Plaza, J.A. De Saja, M.L. Rodriguez-Mendez, Bioelectronic tongue based on lipidic nanostructured layers containing phenol oxidases and lutetium bisphthalocyanine for the analysis of grapes, Biosens. Bioelectron. 57 (2014) 276–283.
[31] H.S. Han, J.-M. You, H. Seol, H. Jeong, S. Jeon, Electrochemical sensor for hydroquinone and catechol based on electrochemically reduced GO–terthiophene–CNT, Sens. Actuators B 194 (2014) 460–469.
[32] L. Wu, L. Feng, J. Ren, X. Qu, Electrochemical detection of dopamine using porphyrin-functionalized graphene, Biosens. Bioelectron. 34 (2012) 57–62.
[33] C. Apetrei, P. Alessio, C.J.L. Constantino, J.A. De Saja, M.L. Rodriguez-Mendez, F.J. Pavinatto, O.N. Oliveira Jr, Biomimetic biosensor based on lipidic layers containing tyrosinase and lutetium bisphthalocyanine for the detection of antioxidants, Biosens. Bioelectron. 26 (2011) 2513–2519.
[34] M.D. Fusco, C. Tortolini, D. Deriu, F. Mazzei, Laccase-based biosensor for the determination of polyphenol index in wine, Talanta 81 (2010) 235–240.